J-PARC UPGRADE

N. Ouchi#, J-PARC Center, JAEA, Tokai, Ibaraki, Japan

Abstract

J-PARC is in the first phase now, which consists of three accelerators; linac, 3-GeV synchrotron, and 50-GeV synchrotron, and three experimental facilities; Materials and Life Science Experimental Facility (MLF), Hadron Experimental Facility, and Neutrino Experimental Facility. Proton beams have reached to the all experimental facilities up to now, and user operation of MLF started in 2008. Superconducting proton linac (SCL) from 400 to 600 MeV and Transmutation Experimental Facility are planned in the second construction phase. SCL will consist of 11 cryomodules and two 9-cell 972 MHz elliptical cavities will be installed in each cryomodule. As two cavities will be driven by one klystron, phase stability between two cavities under the dynamic Lorentz force detuning in the pulsed operation is most important issue to be developed. A prototype cryomodule was fabricated, which was designed to be less Lorentz force detuning. Two-cavity excitation of the cryomodule was tested and phase stability at 2K was confirmed to be safficiently acceptable, while it deteriorated at 4K due to the microphonic noise. Design of SCL and the experimental results of the prototype cryomodule are presented.

INTRODUCTION

The High Energy Accelerator Research Organization (KEK) and the Japan Atomic Energy Agency (JAEA) have been promoting the Japan Proton Accelerator Research Complex (J-PARC) project at the JAEA Tokai site since 2001 [1]. Figure 1 shows an overview of J-PARC, which consists of proton accelerators of a 600-MeV linac, a 3-GeV rapid-cycling synchrotron (RCS), and a 50-GeV main ring synchrotron (MR), as well as experimental facilities of Materials and Life Science Experimental Facility (MLF), Hadron Experimental Facility, Neutrino Experimental Facility, and Transmutation Experimental Facility (TEF). 400-MeV proton beams accelerated by using a normal conducting linac are injected into RCS, which produces proton beams with a nominal power of 1 MW. The 3-GeV proton beams are mainly injected into MLF, in which a pulsed neutron source and a muon source are located, and are partly injected into MR. The proton beams extracted slowly from MR are injected into Hadron Experimental Facility for studies of nuclear and particle physics. Fast extracted beams from MR are injected into Neutrino Experimental Facility, in which intense neutrino beams are shot towards the Super-Kamiokande. 600-MeV proton beams accelerated by using a superconducting linac (SCL) are injected into TEF, in which reactor physics studies and material development are being conducted for an accelerator driven nuclear transmutation system [2]. Therefore, J-PARC is a very challenging and unique research complex for the purposes of neutron science, muon science, nuclear and elementary particle physics, and nuclear engineering with very high intensity proton beams.

#ouchi.nobuo@jaea.go.jp

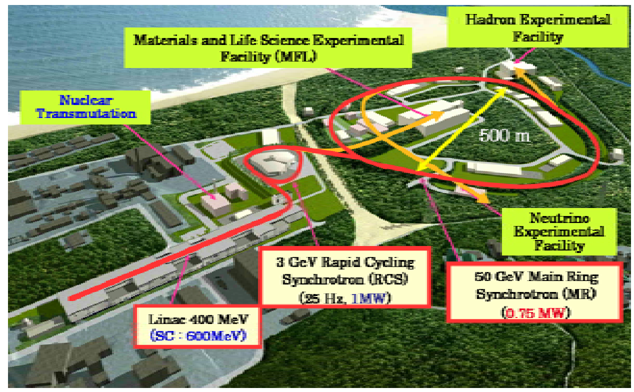

Figure 1: Overview of J-PARC.

The construction of J-PARC is divided into two phases; the J-PARC is in the first phase at the moment, and SCL from 400 to 600 MeV and TEF are in the second construction phase. The higher-energy part of the normal conducting linac in phase-I, which consists of an annular coupling structure (ACS), has been delayed. Therefore, the beam commissioning and operation are being performed at the linac beam energy of 181 MeV, which causes the limited beam power of RCS up to several hundred kW.

This paper provides the J-PARC upgrade program based on SCL in the second construction phase, and R&D results of the cryomodule development for SCL.

STATUS OF J-PARC

Commissioning of J-PARC has been successfully performed on schedule, up to now. The history of the commissioning is summarized in table 1.

The construction started in 2001. Installation of the linac components started in 2005 and the beam commissioning of the linac started in November, 2006. The designed beam energy of 181 MeV was achieved in January, 2007. The beam commissioning of the linac were performed up to June, 2007. In RCS, the first beam injection, circulation, acceleration to 3 GeV and extraction of the 3-GeV beam were successfully performed within only one month in October, 2007. The beam commissioning of RCS was performed up to February, 2008. The first beam injection and circulation in MR were succeeded in May, 2008. The first beam injection to the neutron target in MLF was also succeeded in May, 2008. In September, 2008, high beam power demonstrations were performed at RCS; 210 kW for a period of 70 seconds at 25Hz, and 315kW-equivalent power in one-pulse operation, in which the periods of the powerful beams were limited by the acceptable capacity of the beam dump. The first muon beam was also successfully extracted at MLF in September, 2008. The beam acceleration to 30 GeV in MR was successfully performed in December, 2008. User operation of the MLF neutron beam lines was also started in December, 2008. In January, 2009, slow extracted 30-GeV beam from MR was successfully transported to Hadron Experimental Facility. The beam commissioning of Neutrino Experimental Facility started in April, 2009, and the first neutrino beam production is confirmed by observing the muons by the muon monitor system installed downstream of the neutrino beam line. Upgrade of the linac beam energy to 400 MeV was founded and started in March, 2009, which will complete in 2012.

Table 1: History of J-PARC commissioning

Year	Month	Events
2001	Apr.	Construction started.
2006	Nov.	Linac beam commissioning started.
2007	Jan.	Linac beam energy of 181 MeV was achieved.
	Oct.	RCS beam commissioning started. RCS beam energy of 3 GeV was achieved.
2008	May	MR beam commissioning started. First proton beams reached to the neutron target in MLF.
	Sep.	High beam power demonstration was performed at RCS. First muon beam was extracted in MLF.
	Dec.	User operation of MLF started. MR beam energy of 30 GeV was achieved.
2009	Jan.	First proton beam was transported to the Hadron Experimental Facility.
	Mar.	Energy upgrade of linac to 400 MeV started.
	Apr.	First proton beams reached to the Neutrino target.

SCL FOR J-PARC UPGRADE

This section provides the configuration of the linac and the preliminary conceptual design of SCL.

Configuration of the Linac

Figure 2 shows the schematic configuration of the linac. The linac consists of the front-end part, a drift-tube linac (DTL), a separated-type DTL (SDTL), an ACS linac, and beam transport between the linac and the RCS (L3BT). The front-end part consists of the negative hydrogen ion source, the radio-frequency quadrupole linac (RFQ), low-energy beam transport between the IS and the RFQ, and medium-energy beam transport between the RFQ and the DTL (MEBT). The extraction energies for the IS and the RFQ are 50 keV and 3 MeV, respectively. Chopper cavities for beam chopping, which is necessary for beam injection to RCS, are located in MEBT as well as quadrupole magnets and buncher cavities for beam matching to the following DTL. DTL consists of 3 tanks, and the output energy is 50 MeV. Up to the first DTL tank, the beam commissioning has been successfully carried out at the output beam energy of 20 MeV at the KEK site [3]. SDTL consists of 32 tanks, and the nominal energy is 191 MeV, while the last two tanks are used as debuncher cavities now until the construction of ACS linac. Therefore, the beam commissioning and the operation of J-PARC were started at the linac beam energy of 181 MeV. The ACS part is currently used as a beam transport. As the frequency of the linac up to SDTL is 324 MHz, newly developed klystron and its RF system are in operation in the linac. On the other hand, as triple frequency, 972 MHz, is chosen for ACS, new 972 MHz RF system will be installed in the energy upgrade program to 400 MeV.

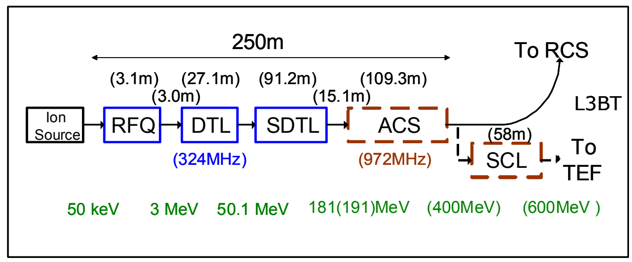

Figure 2: Schematic configuration of the linac.

Main parameters are listed in Table 2. The linac accelerates negative hydrogen, which is converted into proton by charge exchange foils at the injection part of RCS. At the moment, the output energy and the maximum peak beam current of the linac are 181 MeV and 30 mA, respectively, which will be increased to 400 MeV and 50 mA by installing ACS linac and replacing front end part. This upgrade program, which is still phase-I of J-PARC, is necessary to achieve 1 MW beam power at RCS.

Table 2: Main parameters of the linac

Accelerating particle	Negative hydrogen (H^-)
Beam Energy	181 MeV 400 MeV (with ACS linac) 600 MeV (with SCL)
Peak beam current	30 mA (50 mA for 1MW beam power)
Repetition rate	25 Hz (50 Hz in phase-II)
Pulse width	0.5 ms

In phase-II, SCL will be installed to accelerate negative hydrogen beam from 400 to 600 MeV to deliver the beam to TEF. In TEF, most of the 200 kW beams will be injected into the material test facility, and small part of the beam about 10W will be injected into the subcritical assembly to study reactor physics [2]. In phase-I, repetition rate of the normal conducting linac up to 400 MeV is 25 Hz, which will be doubled in phase-II to provide beam to TEF through SCL.

Preliminary Conceptual Design of SCL

Preliminary conceptual design of SCL for J-PARC has been performed [4, 5]. The main parameters of the SCL are listed in Table 3. 9-cell elliptical cavities are used for the beam acceleration, of which frequency is same as that of ACS, 972 MHz. Designed surface peak field is 30 MV/m and corresponding accelerating field is in the range between 9.7 and 11.1 MV/m. The ratio of surface peak field to accelerating field is about 3. Two cavities will be installed in a cryomodule, which is designed to be driven by one klystron to reduce construction cost. Eleven cryomodules are required for beam acceleration between 400 and 600 MeV. This conceptual design is based on the optimum geometrical β, which means geometrical β's are same as the beam β's. If constant geometrical β is applied for all cavities, one more cryomodule or more surface peak field is required. The designed loaded Q is about 500,000, which is lower then the optimum one deduced from the beam loading but leads easier control due to the wider band width. In this condition, total peak RF power is estimated to be about 10 MW.

Table 3: Main parameters of the SCL

Energy	400 – 600 MeV
Frequency	972 MHz
Beam β	0.71 – 0.79
Number of cell per cavity	9
Number of cavity per cryomodule	2
Number of cryomodule	11
Length	58 m
Surface peak field	30 MV/m
Accelerating field	9.7 – 11.1 MV/m
Synchronous phase	-30 degree
Number of klystron	11
Total RF power	10 MW
Loaded Q of cavity	500,000

As for the layout of the SCL, we have currently two options; extend linac in a straight line or bending 90 degree. In a former option, the output beam line of SCL has to turn back towards TEF (see figure 1). On the other hand, the latter option limits the area of TEF. Figure 3 shows the layout of the latter option.

According to the beam dynamics study, required field stability of the cavity is ±1 % in amplitude and ±1 deg. in phase [5]. Pulsed excitation of an elliptical cavity generates dynamic Lorentz force, which leads dynamic detuning and phase change of the cavity [6]. As it is designed that two cavities are driven by one klystron, low level RF can control not each cavity field but vector-sum field of two cavities driven by one klystron. Therefore, stabilization of the RF field in each cavity, especially in phase, is most important issue to be developed to satisfy the beam dynamics requirement.

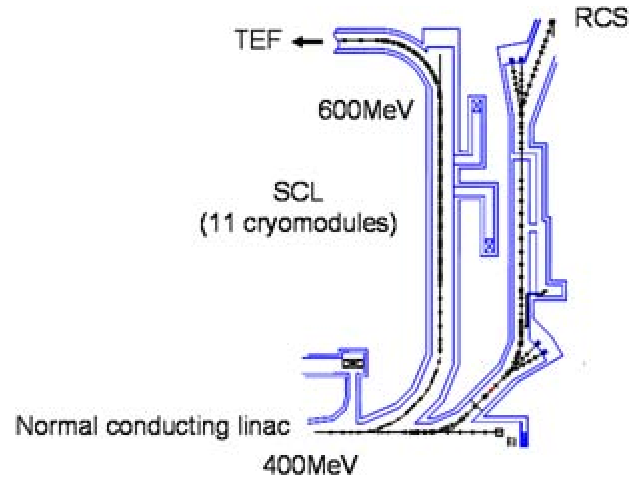

Figure 3: Layout of SCL after bending 90 deg.

Figure 4 shows the design of the 972MHz 9-cell cavity. Inner diameter at iris and equator are 90 and 277 mm, respectively. Beam pipe diameter at input coupler side is enlarged to be 126 mm to achieve enough coupling. Total cell length is about 1 m. In order to reduce the Lorentz force detuning, the wall thickness of the pure niobium cavity is designed to be 4 mm, which is rather thick compared to the common elliptical cavities. The cavity is surrounded by a liquid helium tank made from titanium. As the tuner force is applied between both sides of the bellows of the tank for the cavity tuning, the tank and the tuner system are designed to have enough stiffness to maintain cavity length, which is also effective to reduce the Lorentz force detuning. The calculated static Lorentz force detuning at the surface peak field of 30 MV/m is 131 Hz, of which corresponding detune angle is only 8 deg. by assuming loaded Q of 500,000.

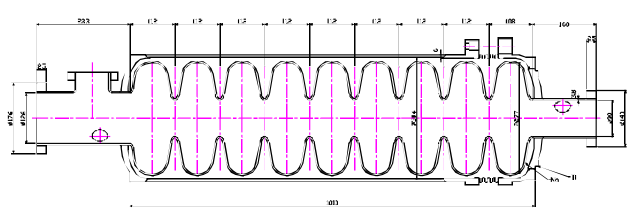

Figure 4: Design of 972MHz 9-cell cavity of β=0.725.

Figure 5 shows the design of the cryomodule. Two input couplers and tuners are located at the central part and outer sides, respectively, which enables stiff tuning system. As operating temperature of the cavity is designed at 2K, a JT-valve is included in the cryomodule. A magnetic shield and thermal shield at 80 K are located just inner side of the vacuum vessel. Thermal intercepts at

5K are also designed between cavity and thermal shield at 80 K to reduce heat leak to the cavities.

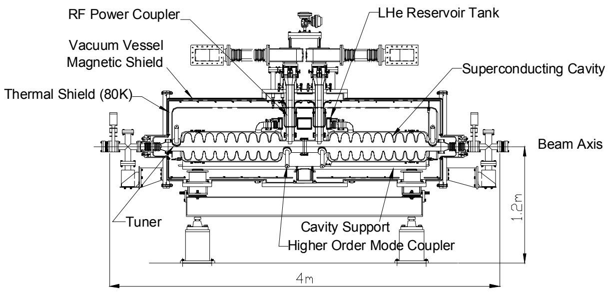

Figure 5: Design of the cryomodule.

DEVELOPMENT OF CRYOMODULE

According to the design of the cavity and cryomodule presented in the previous section, a prototype cryomodule was fabricated. Cryogenic performance, high power test results of the input couplers, RF property of the cavities and horizontal test results with pulsed single-cavity excitation have been already reported [7-11]. Two-cavity excitation by one klystron has been newly performed. This section provides the field performance of the cavity in the vertical and horizontal test and test results of the two-cavity excitation.

Field Performance of the Cavities

Figure 6 shows the vertical test results of the two cavities of β=0.725, which are named "R-Type" and "L-Type" and were installed in the prototype cryomodule. The tests were performed at 2K. The surface peak fields of 32 and 34 MV/m were achieved for R-Type and L-Type cavities, respectively, which were satisfied the target value of 30 MV/m. Obtained quality factors of these cavities at surface peak field at 30 MV/m, more than 10^{10}, were high enough compared to its specification of 5×10^9.

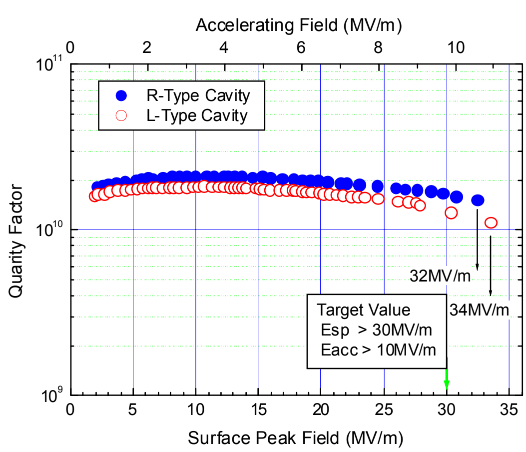

Figure 6: Vertical test results of the two cavities.

As for the horizontal test results, Fig. 7 shows the waveforms of the cavity surface peak field and RF input power for the R-type cavity [10], which are measured at the conditions of operating temperature at 2.1K, repetition rate of 10 Hz and RF pulse width of 3 ms. The surface peak field of 37 MV/m was achieved at the input power at 210 kW as shown in this figure. For the L-Type cavity, the surface peak field of 35 MV/m was achieved. These results satisfied the target value of 30 MV/m. However, in higher repetition rate of 25 Hz, the super-fluid state of the liquid helium was broken due to the large heat leak of the prototype cryomodule [7] and our poor cryogenic performance for evacuation of evaporated helium gas. In a condition of pulse width of 1.5 ms, which is long enough to obtain 0.5 ms flat top for beam acceleration at J-PARC, demonstration of surface peak field of 30 MV/m was successfully performed at the repetition rate of 25 Hz for both cavities.

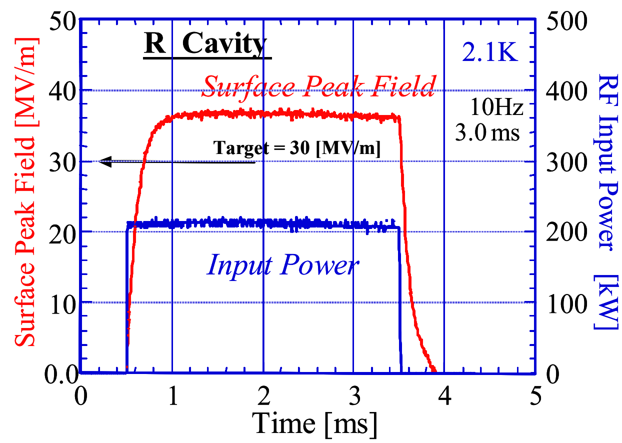

Figure 7: Horizontal test result for R-Type cavity.

Test for Two-cavity Excitation

Two-cavity excitation was tested using a magic-T to feed RF power to both cavities. A 972MHz digital feedback system was used for the low level RF control, which is developed for the ACS cavity. The design of the feedback system is almost same as that used in the current 324-MHz RF system except for the frequency [12, 13]. As it is designed for normal conducting cavity, pulse length is limited up to 1 ms and feedback parameters are not optimized for superconducting cavity.

In the first step of the study, amplitude and phase of the klystron output were stabilized using the digital feedback system in order to observe cavity phase behaviour in a pulsed operation. Figure 8 shows the power and the phase of the klystron output at the pulse width of 1 ms. Except for the rise time up to about 0.2 ms, the amplitude and the phase were confirmed to be well stabilized. Figure 9 shows the accelerating field and phase for both cavities at the repetition rate of 25 Hz. Accelerating fields for the L-Type and the R-Type cavities at the flat top were 9.7 and 10.4 MV/m, respectively. This disagreement is due to the different loaded Q values, 240,000 and 300,000 for the L-Type and the R-Type cavities, respectively. Phase behaviours in a pulse looked almost same for both cavities as shown in Fig. 9.

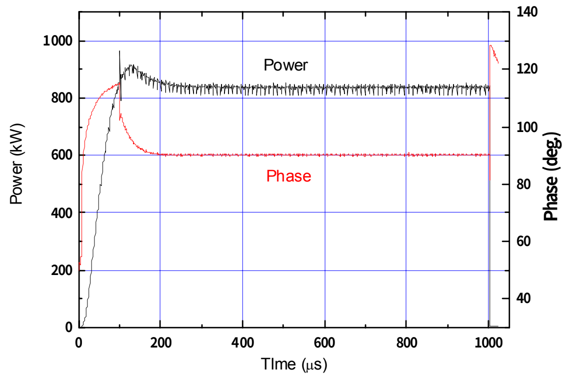

Figure 8: Power and amplitude of the klystron output stabilized by the digital feedback system.

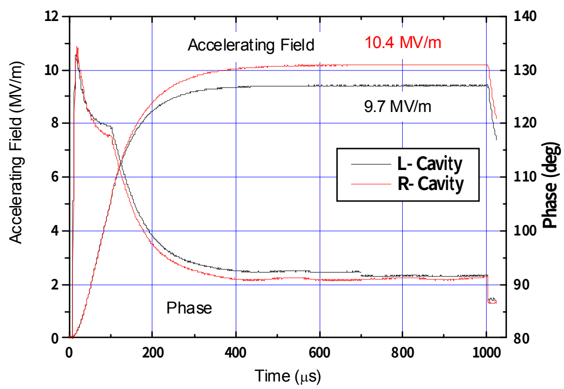

Figure 9: Accelerating field and phase for both cavities.

Figure 10 and 11 shows the 10 waveforms for the each cavity phase taken in about 1 minute at the temperatures of 4.2 K and 2.1 K, respectively. At 4.2 K, cavity phases were scattered about ±5 deg. at the flat top due to microphonic noise as shown in Fig. 10. However, at 2.1 K, cavity phases were well stable within ±1 deg. as shown in Fig. 11. In the experiment at 4.2 K, there was no external vibration source because liquid helium was supplied from dewars. On the other hand, a big vacuum pump was active in the experiment at 2.1 K to evacuate evaporated helium gas, which might generate external vibration. Therefore, the source of the microphonic noise was not from external mechanical vibration but from inside of the cryomodule, which is considered bubbling of the liquid helium. The viscosity of the super-fluid liquid helium is very low and bubbles can flow very smoothly at 2.1 K. These results indicate that the effect of the dynamic Lorentz force detuning is not significant for phase stability due to the design of stiff cavity system and the two-cavity excitation is promising at 2 K to achieve phase stability within ±1 deg.

The phase behaviour at 2 K looks some systematic vibration in Fig. 11. Figure 12 shows the simulation result of the dynamic Lorentz force detuning, where the pulse width is 1.5 ms and not same as this experiment. Frequencies of the dominant mechanical vibration modes are 3.9 and 6.3 kHz, of which deformations are shown in Fig. 13. The cycles of these modes are also shown in Fig. 11. The measured systematic vibration looks consistent with the cycles of the dominant mechanical modes obtained in the simulation.

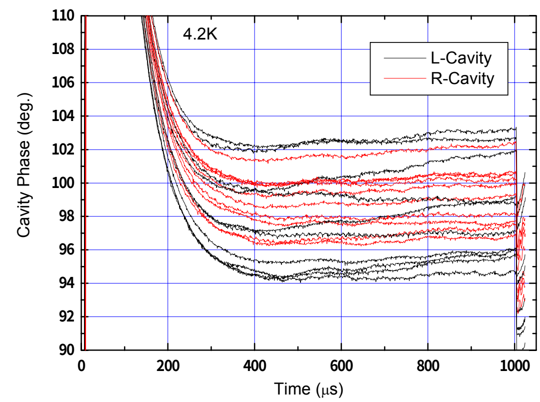

Figure 10: Multi-pulse waveforms for cavity phase at 4.2K.

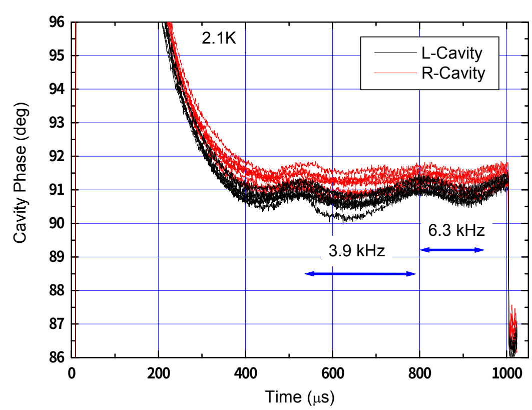

Figure 11: Multi-pulse waveforms for cavity phase at 2.1K.

For the next step, amplitude and phase of the vector sum of two cavities were stabilized using the digital feedback system. Figure 14 shows the 10 waveforms of amplitude and phase for each cavity at 2.1 K, which were also taken in about 1 minute. As the digital feedback system was optimized for the normal conducting cavity, small overshoot was found at the rise time and flat top region was about 0.4 ms, which is not enough to the J-PARC linac beam width of 0.5 ms. A very slow phase shift was also observed in this experiment, of which time constant is in the range of several minutes. This slow phase shift is due to the pressure change of the liquid helium tank and can be stabilized by using a feedback control of the tuner. In spite of them, the results demonstrated sufficient stabilities within ±1 % in amplitude and ±1 deg. in phase in the two-cavity excitation.

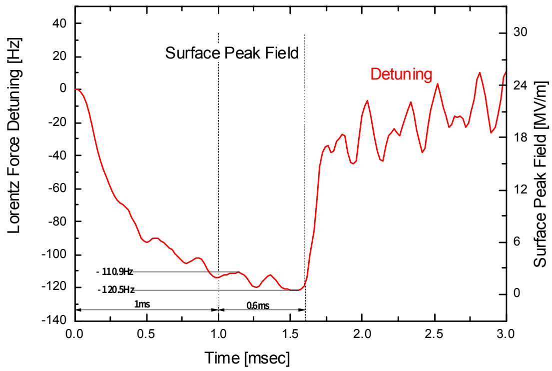

Figure 12: Simulation result for the dynamic Lorentz force detuning.

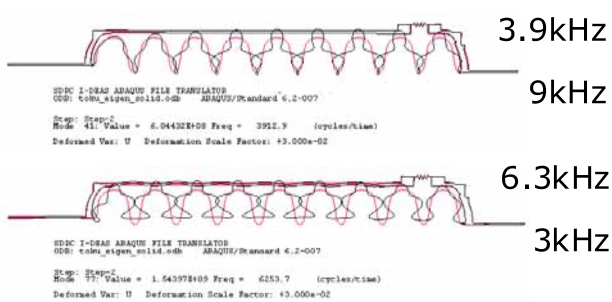

Figure 13: Dominant mechanical vibration modes obtained in the simulation. Red and black lines indicate the original and the amplified deformed cavity shape. The frequencies of the vibration modes are also presented.

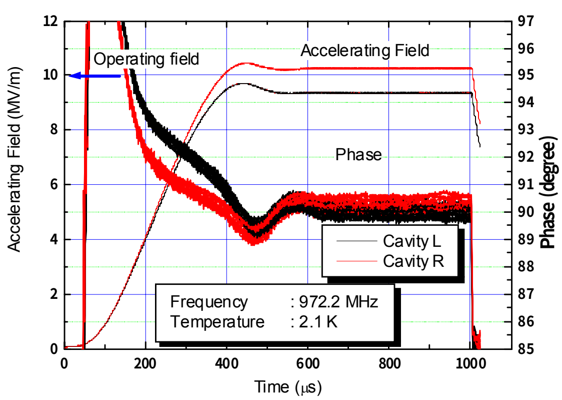

Figure 14: Waveforms of accelerating field and phases for each cavity under the vector sum control.

SUMMARY

Upgrade program is planned in J-PARC using SCL, which accelerates negative hydrogen beams in the energy range between 400 and 600 MeV for the TEF. Preliminary conceptual design of SCL has been already done; it consists of 22 superconducting elliptical cavities and 11 cryomodules. To reduce the construction cost, it is designed that two cavities are driven by one klystron. Under this operating condition, phase stability between these two cavities is most important issue to be developed.

A prototype cryomodule has been developed based on the conceptual design. The field performance of the cavities satisfied the target value of surface peak field of 30 MV/m in both vertical test and horizontal test. Two-cavity excitation was also tested. Due to the design of stiff cavity system, the dynamic Lorentz force detuning is confirmed not to affect the phase stability. On the other hand, it was found that the microphonic noise deteriorates phase stability to be about ±5 deg. at operating temperature of 4.2 K. However, the microphonic noise disappeared at 2.1 K, where phase stability less than ±1 deg. was achieved. In the test of vector sum control, required stabilities within ±1 % in amplitude and ±1 deg. in phase were successfully demonstrated. In this development work, we jumped over the highest hurdle for realization of J-PARC SCL.

REFERENCES

[1] Y. Yamazaki, "The JAERI-KEK Joint Project for the High-Intensity Proton Accelerator, J-PARC", Proc. of PAC 2003, May 12-16, 2003, Portland, USA, p. 576.

[2] T. Sasa, H. Oigawa, K. Tsujimoto, K. Nishihara, K. Kikuchi, Y. Kurata, S. Saito, M. Futakawa, M. Umeno, N. Ouchi, Y, Arai, K. Minato, and H. Takano, Nuclear Engineering and Design 230, 209 (2004).

[3] Y. Kondo, M. Ikegami, T. Kobayashi, T. Ohkawa, and A. Ueno, "Beam Dynamics and Commissioning of the J-PARC Linac", Proc. of ICFA-HB 2004, Bensheim, Germany, p. 79 (2004).

[4] "The Joint Project for High-Intensity Proton Accelerators," JAERI-Tech 99-056 and KEK Report 99-4.

[5] K. Hasegawa, N. Ouchi, K. Mukugi, "System Design of a Superconducting Linac for the High-Intensity Proton Accelerator Project (KEK/JAERI Joint Project)", Proc. of SRF2001, Tsukuba, Japan, p. 607 (2001).

[6] N. Ouchi, "Pulsed SC Proton Linac", Proc. of LINAC2000, Monterey, USA, WE205 (2000).

[7] N. Ohuchi, E. Kako, S. Noguchi, T. Shishido, T. Tsuchiya, A. Akaoka, H. Kobayashi, N. Ouchi, T. Ueno, H. Hara, M. Matsuoka, K. Sennyu and T. Fukano, "Cryogenic Performance of the Prototype Cryomodule for ADS Superconducting Linac", Proc. of EPAC2004, Lucerne, Switzerland, P. 1033 (2004).

[8] E. Kako, S. Noguchi, T. Shishido, H. Asano, E. Chishiro, M. Matsuoka, H. Suzuki and Y. Yamazaki, "High Power RF Test on Input Couplers for 972MHz Superconducting Cavities in the J-PARC Project", Proc. of PAC2003, Portland, USA, P. 1338 (2003).

[9] E. Kako, S. Noguchi, N. Ohuchi, T. Shishido, A. Akaoka, H. Kobayashi, N. Ouchi, T. Ueno, H. Hara,

M. Matsuoka and K. Sennyu, "RF Property of the Prototype Cryomodule for ADS Superconducting Linac", Proc. of EPAC2004, Lucerne, Switzerland, P. 1033 (2004).

[10] E. Kako, S. Noguchi, N. Ohuchi, T. Shishido, T. Tsuchiya, A. Akaoka, E. Chishiro, T. Hori, H. Kobayashi, M. Nakata, N. Ouchi and Y. Yamazaki, "High Power Test of the Prototype Cryomodule for ADS Superconducting Linac", Proc. of PAC2005, Knoxville, USA, P. 3579 (2005).

[11] E. Kako, S. Noguchi, N. Ohuchi, T. Shishido, T. Tsuchiya, A. Akaoka, E. Chishiro, T. Hori, H. Kobayashi, M. Nakata, N. Ouchi and Y. Yamazaki, "Pulsed Operation of the 972 MHz Prototype Cryomodule for ADS Superconducting Linac", Proc. of SRF2005, Ithaca, USA, ThP30 (2005).

[12] Z. Fang, S. Anami, S. Michizono, S. Yamaguchi, T. Kobayashi, and H. Suzuki, "RF Feedback control systems of the J-PARC Linac," Proc. of PAC2007, Albuquerque, USA, p. 2101 (2007).

[13] T. Kobayashi, E. Chishiro, T. Hori, H. Suzuki, M. Yamazaki, S. Anami, Z. Fang, Y. Fukui, M. Kawamura, S. Michizono, K. Nanmo, and S. Yamaguchi, "Performance of J-PARC Linac RF System," Proc. of PAC2007, Albuquerque, USA, p. 2128 (2007).